Available online at www.sciencedirect.com
SCIENCE DIRECT®
Advances in Space Research 37 (2006) 2263–2268
ADVANCES IN SPACE RESEARCH (a COSPAR publication)
www.elsevier.com/locate/asr

First results of ozone profiles between 35 and 65 km retrieved from SCIAMACHY limb spectra and observations of ozone depletion during the solar proton events in October/November 2003

G.J. Rohen [a,*], C. von Savigny [a], E.J. Llewellyn [b], J.W. Kaiser [c], K.-U. Eichmann [a], A. Bracher [a], H. Bovensmann [a], J.P. Burrows [a]

[a] Institute of Environmental Physics (IUP), University of Bremen, Otto-Hahn-Allee 1, 28359 Bremen, Germany
[b] Institute of Space and Atmospheric Studies, University of Saskatchewan, 116 Science Place, Saskatoon, Canada S7N 5E2
[c] Remote Sensing Laboratories (RSL), University of Zurich, Winterthurer Str. 190, 8057 Zurich, Switzerland

Received 19 October 2004; received in revised form 11 March 2005; accepted 12 March 2005

Abstract

Ozone density profiles between 35 and 65 km altitude are derived from scattered sunlight limb radiance spectra measured by the SCIAMACHY instrument on the Envisat satellite. The method is based on the inversion of normalized limb radiance profiles in the Hartley absorption bands of ozone at selected wavelengths between 250 and 310 nm. It employs a non-linear Newtonian iteration version of Optimal Estimation (OE) coupled with the radiative transfer model SCIARAYS. The limb scatter technique combined with a classical OE retrieval in the short-wave UV-B and long-wave UV-C delivers reliable results as shown by a first comparison with MIPAS V4.61 profiles yielding agreement within 10% between 38 and 55 km. An overview of the methodology and an initial error analysis are presented. Furthermore the effect of the solar proton storm between 28 October and 6 November 2003 on the ozone concentration profiles is shown. They indicate large depletion of ozone of about 60% at 50 km in the Northern hemisphere, a weaker depletion in the Southern hemisphere and a dependence of the depletion on the Earth's magnetic field.

Keywords: SCIAMACHY; Ozone; Mesosphere; Retrieval technique; Solar proton event October 2003

1. Introduction

Emission and absorption spectroscopy are two techniques used to retrieve ozone profiles in the mesosphere: a common technique uses the airglow emissions of oxygen (Noxon, 1975; Llewellyn and Witt, 1977; Marsh et al., 2002, 2003). Another technique is the absorption spectroscopy by stellar occultation, e.g., Global Ozone Monitoring by Occultation of Stars (GOMOS) (Kyrölä, 2004), solar occultation, e.g., Halogen Occultation Experiment (HALOE) (Russell et al., 1993) or by scanning the limb of the Earth, e.g., Optical Spectrometer and InfraRed Imager System (OSIRIS) (Llewellyn et al., 2004). Rusch et al. (1984) have been the first to retrieve ozone profiles from limb scatter observations. They used UV limb radiance profile measurements at 265.0 and 296.4 nm performed with an ultraviolet spectrometer on the Solar Mesosphere Explorer (SME) to infer ozone concentrations between about 48 and 65 km.

The significant absorption of solar radiation in the Hartley bands of ozone alters the UV limb radiance profiles within the 35–65 km tangent height range. Measurements of limb scattered radiance profiles can therefore be used to retrieve ozone concentrations in the upper stratosphere and lower mesosphere, if the selection of the wavelengths is done carefully.

* Corresponding author. Tel.: +49 421 218 4352; fax: +49 421 218 4555.
E-mail address: rohen@iup.physik.uni-bremen.de (G.J. Rohen).

0273-1177/$30
doi:10.1016/j.asr.2005.03.160

2. SCIAMACHY on Envisat

The European Space Agency's (ESA) spacecraft Environmental satellite (Envisat) was launched on 1 March 2002 from Kourou (French Guiana) into a sun-synchronous polar orbit with an inclination angle of 98.55° and a descending equator crossing local time of 10:00 am. SCanning Imaging Absorption SpectroMeter for Atmospheric CartograpHY (SCIAMACHY) (Bovensmann et al., 1999), one of the ten instruments on Envisat, is a spectrometer designed to measure transmitted, reflected and scattered sunlight in the wavelength region from 214 to 2380 nm at a moderate spectral resolution of 0.24–1.48 nm. The instrument consists of eight grating spectrometers and photo-diode array detectors. It measures the daylight radiance in limb and nadir viewing geometry, and also solar or lunar light transmitted through the atmosphere in occultation mode. In limb mode the instantaneous field of view of SCIAMACHY is 0.045° in elevation (about 2.6 km at the tangent point) and 1.8° in azimuthal direction (about 110 km). A typical limb scan cycle comprises 31 horizontal scans from the Earth's surface to 92 km with a duration of 1.5 s each. During a typical limb cycle duration the spacecraft moves about 400 km in the along-track direction. The instrument reaches global coverage within 6 days.

3. Retrieval method

The method used to recover ozone density profiles from SCIAMACHY observations follows that employed by Flittner et al. (2000) and McPeters et al. (2000) to retrieve ozone density profiles from the LORE/SOLSE limb scatter measurements in the Huggins absorption bands of ozone. A similar method, using the Chappuis bands of ozone, has been applied to retrieve stratospheric ozone profiles, e.g., from OSIRIS (von Savigny et al., 2003) and SCIAMACHY limb scattering observations, using three combined wavelengths (Eichmann et al., 2004; von Savigny et al., 2004b).

Fig. 1 shows the weighting functions for four selected wavelengths. They show the sensitivity of the wavelength dependent radiance profiles at each tangent height with respect to ozone concentrations. The figures show that there is no sensitivity below 35 km at wavelengths shorter than 310 nm. Currently the retrieval version V2.16 is run with 250, 252, 254, 264, 267.5, 273.5, 283, 286.5, 288, 290, 305, 307 and 310 nm simultaneously by averaging the radiances over 2 nm wavelength intervals. The wings of Fraunhofer lines and dayglow emissions are avoided. Expected emissions are the NO-γ bands ($A^2\Sigma^+ \rightarrow X^2\Pi$), which are the most prominent emission features in the UV, the N_2 Vegard–Kaplan bands ($A^3\Sigma_u^+ \rightarrow X^1\Pi_g^+$), the N_2 second positive bands ($C^3\Pi_u \rightarrow B^3\Sigma_g$), atomic oxygen lines ($^2P \rightarrow {}^4S$) at 247.000 and 247.109 nm and ($^1S \rightarrow {}^3P$) at 297.2 nm (López-Puertas, 2000). Other expected emissions from iron, sodium and magnesium can hardly be seen. Only the NO-γ bands play an important role.

The first step of the retrieval scheme consists of normalization of the limb radiance profiles

$$I^n_{i,k} = \frac{I_{i,k}}{I_{i,\mathrm{ref}}}, \tag{1}$$

with $I_{i,k}$ denoting the limb radiance at wavelength λ_i, $i \in \{1, \ldots, 13\}$ and tangent height Th_k, $k \in \{1, \ldots, 21\}$. $I_{i,\mathrm{ref}}$ denotes the radiance at wavelength λ_i at the chosen reference tangent height. Each reference height is chosen at altitudes between 56 and 70 km. The effect of normalization is (a) to reduce the sensitivity to all disturbances which affect all wavelengths, e.g., clouds, and (b) that absolute calibration errors cancel out. Therefore the

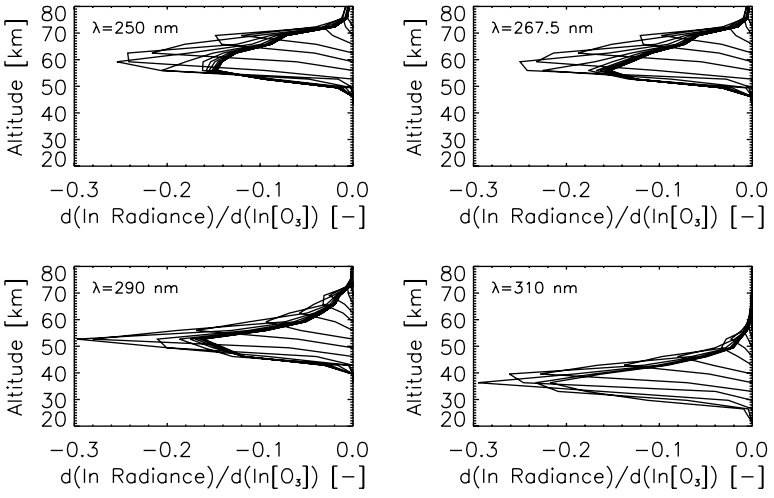

Fig. 1. Weighting functions of a sample ozone profile retrieval for four selected wavelengths, which show the sensitivity of the retrieval method from 35 to 65 km. Each curve represents the fractional sensitivity for a different tangent height from 20 to 80 km. The measurement was made on 12 March 2003. The solar zenith angle is 78.9°.

normalization at wavelength-dependent tangent heights minimizes the possible impact of several error sources. The normalized radiance profiles are combined to a column vector $\mathbf{y} = (I^n_{i,k})^{\mathrm{T}}$. A non-linear Newton iteration scheme of OE is used with the program package SCIARAYS, which has been developed especially for the retrieval of trace gas concentrations from UV and visible (UV–vis) limb measurements (Kaiser, 2001). It contains a radiative transfer model and an instrument model and solves the integral form of the radiative transfer equation using fully spherical ray tracing, optional refractive bending and double-scattering. Weighting functions are derived analytically. Fig. 2 shows a fit of the modelled radiances for four selected wavelengths and the residuals for all wavelengths for a sample profile retrieval. Ozone absorbs very strongly in the Hartley bands, and model simulations showed, that surface reflection is negligible and multiple-scattering below 310 nm contributes less than 5% and below 305 nm less than 1% to the radiances. Thus the reflected, the first reflected and then scattered radiation, and the second scattered radiation can be neglected.

The used temperature and pressure climatology is a compilation of several experimental datasets and model data (McPeters, 1993). The a priori ozone profiles for the inversion scheme are taken from the United Kingdom Universities Global Atmospheric Modelling Programme (UGAMP) climatology based on five years of averaged SME, Stratospheric Aersol and Gas Experiment II (SAGE II), and Solar Backscatter Ultra-Violet (SBUV) satellite data (Li and Shine, 1995). An a priori error of 80% was assumed and the a priori covariance matrix was assumed to be diagonal. The measurement error was estimated at 6%. Averaging kernels, which show, how the retrieved profiles dependent on the true profile, and the vertical resolution of a sample profile retrieval can be seen in Fig. 3.

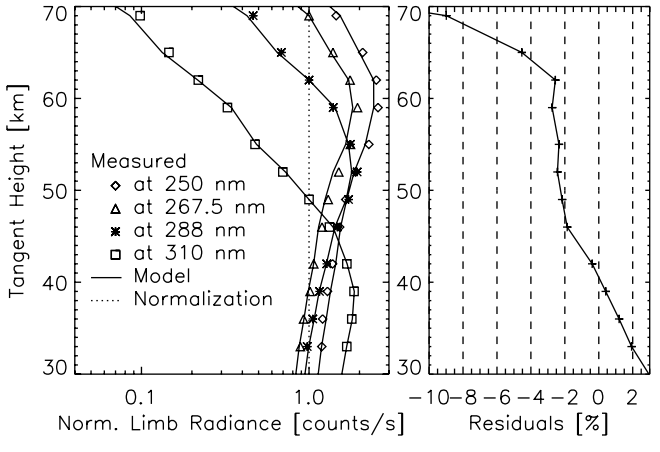

Fig. 2. (Left panel) Newton iteration fit of measured to modelled radiances at four wavelengths for the same sample profile retrieval as in Fig. 1. The dotted line indicates the normalization points. The normalization point of the measurement at 250 nm is located at 76 km and cannot be seen in this figure. (Right panel) Corresponding residual for all wavelengths is below 3%, except above 62 km, where they exceed more than 5%.

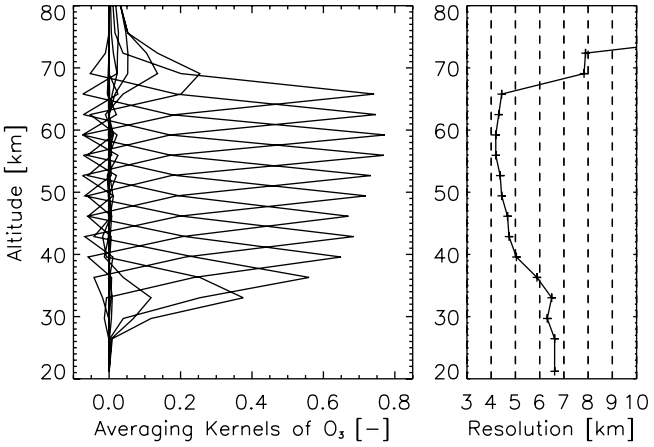

Fig. 3. Averaging kernels and calculated vertical resolution of a retrieved profile, as given by the Full Width at Half Maximum (FWHM) of the averaging kernels obtained from a sample ozone profile retrieval (same observation as in Figs. 1 and 2). The resolution between 40 and 65 km is less than 5 km.

4. Error statistics

An overview of the relevant sources of error is given in Table 1. The largest error source is the residual pointing error of the Envisat orbit model propagator (von Savigny et al., 2005). To correct the tangent heights and therefore minimize the errors, a pointing retrieval using the *knee-technique* (Janz et al., 1996) was performed (Kaiser et al., 2004). This reduces the pointing precision from previously up to 3.5–0.3 km after the pointing-retrieval (von Savigny et al., 2005). With an assumed accuracy of the tangent heights of 0.5 km the estimated errors in the ozone profiles due to the tangent height inaccuracy are between 4 and 19%.

Table 1
Overview of error sources (%)

Altitude	35 km	39 km	45 km	51 km	57 km	65 km
Single scattering[a]	3	1	0.3	0.1	0.1	0.05
A priori[b]	12	1	3	2.5	3	7
Ground albedo (A)[c]	2	0.6	0.1	0.02	0.01	0.01
Background density[d]	0.7	1.2	0.7	0.2	0.1	0.1
Temperature[e]	10	7	3	2	1	3
Pointing errors[f]	4	10	15	16	17.5	19
Solar zenith angle[g]	0.6	0.3	0.4	0.5	0.3	0.2
Solar zenith angle[h]	12	10	9	10	9	7
Cross-sections[i]	4	7	5	2	1	2

[a] Neglecting multiple scattering and reflection.
[b] Change of 100%.
[c] Changing from $A = 0$ to $A = 0.5$.
[d] 20% decrease.
[e] $\Delta T = 40$ K.
[f] $\Delta h = 0.5$ km.
[g] Changing from 50° to 48°.
[h] Changing from 84° to 82°.
[i] Temperature-dependent, $\Delta T = 40$ K.

Additionally, mesospheric clouds, which occur at about 83 km at high latitudes in the summer hemisphere (von Savigny et al., 2004a) are detected with an algorithm and the affected measurements are rejected.

4.1. Comparison with MIPAS results

The Michelson Interferometer for Passive Atmospheric Sounding (MIPAS) (Fischer and Oelhaf, 1996) is a Fourier Transform Spectrometer (FTS) operating in limb-geometry in the infrared region from 4.15 to 14.6 μm with a high spectral resolution. The MIPAS operational products are provided by ESA and validated with ozone profiles, e.g., from HALOE (V19) and SAGE II (V6.2) (Bracher et al., 2004), where the ozone profiles differ by about 5–15% from HALOE and SAGE II profiles. The validation in the work of (Bracher et al., 2004) is restricted to altitudes from about 12–60 km, thus a validation with MIPAS only can give reasonable validation results with SCIAMACHY (V2.16) ozone profiles up to 60 km. While the MIPAS ozone concentrations are in general 2–15% higher than ozone concentrations from HALOE, the SCIAMACHY ozone concentrations in the altitude region from 38 to 55 km are about 10% lower than MIPAS and 20% less below and above this limits (see Figs. 4 and 5).

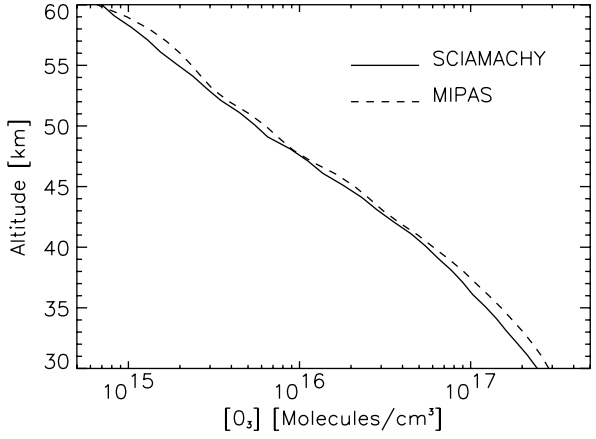

Fig. 4. Comparison of mean ozone profiles retrieved from all 434 local coincident SCIAMACHY V2.16 and MIPAS V4.61 measurements in March, 2004. The local coincidence of the particular MIPAS measurement is within 500 km radius around the SCIAMACHY tangent point and is further restricted to 2° difference in the solar zenith angles.

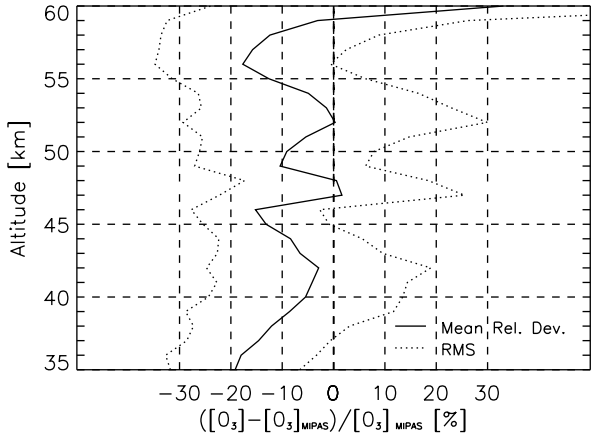

Fig. 5. Validation statistics of mean ozone profiles retrieved from SCIAMACHY limb spectra in comparison to the 434 collocated operational MIPAS V4.61 ozone profiles of March, 2004. The coincidence criteria are the same as in Fig. 4. Except for an altitude of 45 km the mean relative deviation is below 10% in altitudes from 37 to 55 km. The ranges above and below exceed deviations of 20%.

5. Ozone depletion during the Solar Proton Event (SPE) in October/November 2003

Between 28 October 2003 and 4 November 2003 the largest solar flares of the solar cycle 23 to date occurred causing a big particle and radiation storm on Earth. Depletion of ozone by an SPE was first observed by Weeks et al. (1972). Swider and Kenesha (1973) suggested the production of odd hydrogen as a cause of the observed ozone depletion. Crutzen and Solomon (1980) and Solomon and Crutzen (1981) gave the first reasonable model predictions to explain the mechanism for the ozone depletion observed with SME. Another detailed observation of the SPE on 13 July, 1982 (Thomas et al., 1983) with SME has been discussed by Solomon et al. (1983): highly energetic protons ionize the air and produce HO_x and NO_x constituents through complicated water cluster chemistry. HO_x is responsible for the depletion during the first days, while NO_x can have an effect over months or longer and

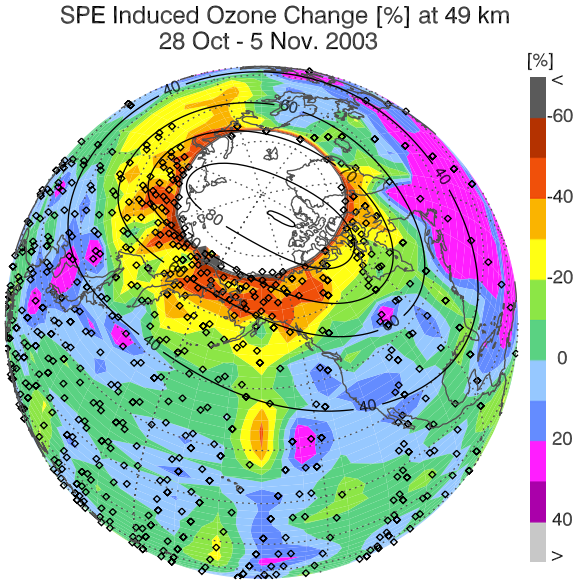

Fig. 6. Ratio of averaged ozone concentrations at an altitude of 49 km in the Northern hemisphere during the SPE (28 October to 6 November) and during a reference period (20–24 October) before the SPE. The isolines of magnetic inclination (black lines) were produced by the World Magnetic Model (WMM) (Macmillan and Quinn, 2000). The diamonds indicate the locations of SCIAMACHY limb scattering observations. The polar region in the Northern hemisphere is not covered by SCIAMACHY limb scatter observations due to an inclination angle of 98.55°, and because the Pole is not sunlit in early November.

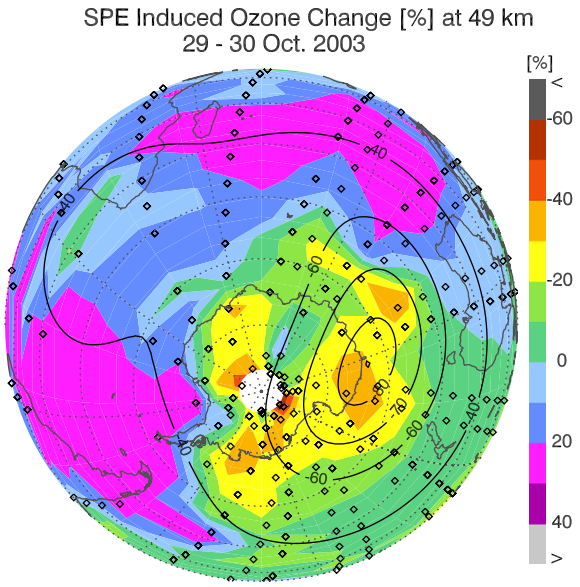

Fig. 7. In the Southern hemisphere, evident changes of the ozone concentrations can only be observed in a period from 29 to 30 October 2003. The ozone depletion is mainly located where the solar particles penetrate the atmosphere at the magnetic poles. Descriptions are the same as in Fig. 6.

can be transported downward into the stratosphere (Crutzen et al., 1975). A newer review of the investigations can be found, e.g., in Jackman and McPeters (2004).

In limb viewing geometry SCIAMACHY observes at tangent points which are about 3000 km away from the sub-satellite point, so the impact of radiation hits on the analysed ozone profiles is reduced. In the dataset no indications of radiation hits which may affect the profile retrieval were found.

Figs. 6 and 7 show the depletion of ozone at 49 km in the Northern and Southern hemisphere. In the Southern hemisphere the ozone depletion can only be seen clearly during the first part of the event from 29 to 30 October. In contrast to the observations in the Southern hemisphere, the depletion in the north is stronger and can be seen over the whole particle precipitation period from 28 October to 7 November 2003. The hemispheric difference is in part due to a different ambient HO_x production, which is a consequence of the differences in the solar zenith angles. More ambient (not SPE produced) HO_x is present in the Southern hemisphere, leading to lower ambient ozone levels. Therefore the impact of the SPE produced HO_x will relatively not be as severe. A clear correlation of the ozone depletion and the strength of the Earth's magnetic field is observed (see Fig. 7 and explanations in the caption of Fig. 6).

6. Conclusions

The retrieval version V2.16 of upper stratospheric/lower mesospheric ozone profiles with thirteen selected wavelengths in the Hartley bands of ozone provides reliable profiles of ozone concentrations from 35 to 65 km. A first validation with ozone profiles retrieved from the MIPAS instrument shows a good agreement. The main error sources of the retrieved ozone profiles have been estimated. Furthermore we described the ozone depletion caused by the SPE at the end of October and in the beginning of November 2003 with maxima of about 60% in the Northern hemisphere and of about 40% in the Southern hemisphere. In the Southern hemisphere a correlation of the ozone depletion and the Earth's magnetic field was observed.

Acknowledgements

Parts of this work have been funded by the German Ministry of Education and Research BMBF (Grant 07UFE12/8) and the German Aerospace Centre DLR (Grant 50EE0027). We would also like to thank ESA for providing the operational MIPAS ozone profiles for validation.

References

Bovensmann, H., Burrows, J.P., Frerick, J., Noël, S., Rozanov, V.V., Chance, K.V., Goede, A.P.H. SCIAMACHY: mission objectives and measurements modes. J. Atmos. Sci. 56 (2), 127–148, 1999.

Bracher, A., Bramstedt, K., Sinnhuber, M., Weber, M., Burrows, J.P. Validation of MIPAS O_3, NO_2, H_2O and CH_4 profiles (V4.61) with collocated measurements of HALOE and SAGE II, in: ESA Second Workshop on the Atmospheric Chemistry Validation of ENVISAT (ACVE-2), Frascati, Italy. SP-562. Nordwijk, Netherlands, p. 319, 2004.

Crutzen, P.J., Isaksen, I.S.A., Reid, G.C. Solar proton events: stratospheric sources of nitric oxide. Science 189, 457–458, 1975.

Crutzen, P.J., Solomon, S. Response of mesospheric ozone to particle precipitation. Planet. Space Sci. 28, 1147–1153, 1980.

Eichmann, K.-U., Kaiser, J.W., von Savigny, C., Rozanov, A., Rozanov, V.V., Bovensmann, H., König, M. v., Burrows, J.P. SCIAMACHY limb measurements in the UV/Vis spectral region: first results. Adv. Space Res. 34 (4), 744–748, 2004.

Fischer, H., Oelhaf, H. Remote sensing of vertical profiles of atmospheric trace constituents with MIPAS limb-emission spectrometers. Appl. Opt. 35 (16), 2787–2796, 1996.

Flittner, D.E., Bhartia, P.K., Herman, B.M. O_3 profiles retrieved from limb scatter measurements: theory. Geophys. Res. Lett. 27 (17), 2601–2604, 2000.

Jackman, C.H., McPeters, R.D. The effect of solar proton events on ozone and other constituents, in: Solar Variability and its Effects on Climate. No. 10.1029/141GM21. American Geophysical Union, pp. 305–319, 2004.

Janz, S.J., Hilsenrath, E., Flittner, D., Heath, D. Rayleigh scattering attitude sensor. Proc. Spie 2831, 146–153, 1996.

Kaiser, J.W. Atmospheric parameter retrieval from UV–vis-NIR limb scattering measurements. Ph.D. thesis, University of Bremen, 2001.

Kaiser, J.W., von Savigny, C., Eichmann, K.-U., Noël, S., Bovensmann, H., Burrows, J.P. Satellite-pointing retrieval from atmospheric limb-scattering of solar UV-B radiation. Can. J. Phys. 82, 1041–1052, 2004.

Kaufmann, M.O., Gusev, O.A., Grossmann, K.U., Martin-Torres, F.J., Marsh, D.R., Kutepov, A.A. Satellite observations of daytime and nighttime ozone in the mesosphere and lower thermosphere. J. Geophys. Res. 108 (D9), 4272–4285, 2003.

Kyrölä, E., Tamminen, J., Leppelmeier, G.W., Sofieva, V., Hassinen, S., Bertaux, J.L., Hauchecorne, A., Dalaudier, F., Cot, C., Korablev, O., d'Anton, O.F., Barrot, G., Mangin, A., Théodore, B., Guirlet, M., Etanchaud, F., Snoeij, P., Koopman, R., Saavedra, L., Fraisse, R., Fussen, D., Vanhellmont, F. GOMOS on Envisat: an overview. Adv. Space Res. 33 (7), 1020–1028, 2004.

Li, D., Shine, K.P. A 4-dimensional ozone climatology of ozone for UGAMP models. UGAMP internal report 35, British Geological Survey, Department of Meteorology, University of Reading, 1995.

Llewellyn, E.J., Lloyd, N.D., Degenstein, D.A., Gattinger, R.L., Petelina, S.V., Bourassa, A.E., Wiensz, J.T., Ivanov, E.V., McDade, I.C., Solheim, B.H., McConnell, J.C., Haley, C.S., von Savigny, C., Sioris, C.E., McLinden, C.A., Evans, W.F.J., Puckrin, E., Strong, K., Wehrle, V., Hum, R.H., Kendall, D.J.W., Matsushita, J., Murtagh, D.P., Brohede, S., Stegman, J., Witt, G., Barnes, G., Payne, W.F., Piché, L., Smith, K., Warshaw, G., Deslauniers, D.-L., Marchand, P., Richardson, E.H., King, R.A., Wever, I., McCreath, W., Kyrölä, E., Oikarinen, L., Leppelmeier, G.W., Auvinen, H., Mégie, G., Hauchcorne, A., Lefévre, F., de La Nöe, J., Ricaud, P., Frisk, U., Sjoberg, F., von Schéele, F., Nordh, L. The OSIRIS instrument on the Odin spacecraft. Can. J. Phys. 82 (6), 411–422, 2004.

Llewellyn, E.J., Witt, G. The measurements of ozone concentrations at high latitudes during the twilight. Planet. Space Sci. 25 (2), 165–172, 1977.

López-Puertas, M. Definition of observational requirements for support to a future Earth explorer atmospheric chemistry mission. Tech. Rep. ESTEC Contract Number 13048/98/NL/DG, WP 6000: Molecular Non-Local Thermodynamic Equillibrium Working Document V2.0, Instituto de Astrofisica de Andalucia (CSIC), Granada, Spain, 2000.

Macmillan, S., Quinn, J.M., The derivation of World Magnetic Model 2000. Tech. Rep. WM/00/17R, British Geological Survey, Edinburgh, 2000.

Marsh, D.R., Skinner, W.R., Marshall, A.R., Hays, P.B., Ortland, D.A., Yee, J.-H. High Resolution Doppler Imager observations of ozone in the mesosphere and lower thermosphere. J. Geophys. Res. 107 (D19), 4390, 2002.

McPeters, R. Ozone profile comparisons, in: The atmospheric effects of stratospheric aircraft: Report of the 1992 models and measurement workshop. No. 1292 in NASA Reference Publ. M.J. Prather, E.E. Remsberg, pp. D31–D37, 1993.

McPeters, R.D., Janz, S.J., Hilsenrath, E., Brown, T.L., Flittner, D.E., Heath, D.F. The retrieval of O_3 profiles from limb scatter measurements: results from the Shuttle Ozone Limb Sounding Experiment. Geophys. Res. Lett. 27 (17), 2597–2600, 2000.

Noxon, J.F. Twilight enhancements in $O_2(b^1\Sigma_g)$ emission. J. Geophys. Res. 80, 1370–1373, 1975.

Rusch, D.W., Mount, G.H., Barth, C.A., Thomas, R.J., Callan, M.T. Solar Mesosphere Explorer Ultraviolet Spectrometer: Measurements of ozone in the 1.0-0.1 mbar region. J. Geophys. Res. 89 (D7), 11677–11687, 1984.

Russell, J.M., Tuck, A.F., Gordley, L.L., Park, H.H., Drayson, S.R., Hesketh, D.H., Cicerone, R.J., Frederick, J.E., Harries, J.E., Crutzen, P.J. The Halogen Occultation Experiment. J. Geophys. Res. 98 (D6), 10777–10797, 1993.

Solomon, S., Crutzen, P.C. Analysis of the August 1972 solar proton event including chlorine chemistry. J. Geophys. Res. 86, 1140–1146, 1981.

Solomon, S., Reid, G.C., Rusch, D.W., Thomas, R.J. Mesospheric ozone depletion during the solar proton event of July 13, 1982. Part II. Comparison between theory and measurements. Geophys. Res. Lett. 10, 257–260, 1983.

Swider, W., Kenesha, T.J. Decrease of ozone and atomic oxygen in the lower mesosphere during a PCA event. Planet. Space Sci. 21, 1969, 1973.

Thomas, R.J., Barth, C.A., Rottman, G.J., Rusch, D.W., Mount, G.H., Lawrence, G.M. Ozone densities in the mesosphere (50-90 km) measured by the SME limb scanning near infrared spectrometer. Geophys. Res. Lett. 20, 245, 1983.

von Savigny, C., Haley, C.S., Sioris, C.E., McDade, I.C., Llewellyn, E.J., Degenstein, D., Evans, W.F.J., Gattinger, R.L., Griffioen, E., Kyrölä, E., Lloyd, N.D., McConnell, J.C., McLinden, C.A., Mégie, G., Murtagh, D.P., Solheim, B., Strong, K. Stratospheric ozone profiles retrieved from limb scattered sunlight radiance spectra measured by the OSIRIS instrument on the Odin satellite. Geophys. Res. Lett. 30 (14), 1755, 2003.

von Savigny, C., Kaiser, J.W., Bovensmann, H., Burrows, J.P., McDermind, I.S., Leblanc, T. Spatial and temporal characterization of SCIAMACHY limb pointing errors during the first three years of the mission. Atmos. Chem. Phys. 5, 2593–2602, 2005.

von Savigny, C., Kokhanovsky, A., Bovensmann, H., Eichmann, K.-U., Kaiser, J., Noël, S., Rozanov, A.V., Skupin, J., Burrows, J.P. NLC detection and particle size determination: first results from SCIAMACHY on Envisat. Adv. Space Res. 34, 851–856, 2004a.

von Savigny, C., Rozanov, A., Bovensmann, H., Eichmann, K.-U., Noël, S., Rozanov, V.V., Sinnhuber, B.-M., Weber, M., Burrows, J.P. The ozone hole break-up in September2002 as seen by SCIAMACHY on ENVISAT. J. Atmos. Sci. 62 (3), 721–734, 2004b.

Weeks, L.H., Chuikay, R.S., Corbin, J.R. Ozone measurements in the mesosphere during the solar proton event of 2 November 1969. J. Atmos. Sci. 29, 1138–1142, 1972.